The Journal of Infectious Diseases

SUPPLEMENT ARTICLE

In Situ Imaging of Fluorescent Nipah Virus Respiratory and Neurological Tissue Tropism in the Syrian Hamster Model

Stephen R. Welch, Florine E. M. Scholte, Jessica R. Harmon, JoAnn D. Coleman-McCray, Michael K. Lo, Joel M. Montgomery, Stuart T. Nichol, Christina F. Spiropoulou, and Jessica R. Spengler

Viral Special Pathogens Branch, Division of High-Consequence Pathogens and Pathology, Centers for Disease Control and Prevention, Atlanta, Georgia

Using a recombinant Nipah virus expressing a fluorescent protein (ZsG), we visualized virus tropism in the Syrian hamster model. We found that anatomical localization of fluorescence correlated to clinical signs; signal was primarily visualized in the respiratory tract in animals with acute-onset terminal disease, whereas central nervous system localization was seen in animals that succumbed with delayed disease onset. While polymerase chain reaction (PCR) detection corresponded well to ZsG signal, virus was only isolated from some lung, brain, liver, and kidney samples that were ZsG and/or PCR positive, and only from animals euthanized on or before 15 days post infection.

Keywords. Nipah virus; henipavirus; ZsGreen1; Syrian golden hamster; in situ fluorescent imaging; lung; brain; central nervous system; neurological; respiratory.

Nipah virus (NiV; family *Paramyxoviridae*, genus *Henipavirus*), first recognized in Malaysia and Singapore in 1998, causes a range of clinical signs from asymptomatic infection to acute respiratory illness and fatal encephalitis. The virus is maintained in nature by pteropid bats (flying foxes) and circulates in a variety of pteropid species over a wide geographical area, including Malaysia, Bangladesh, India, Papua New Guinea, Cambodia, Indonesia, and Thailand [1].

Patients develop symptoms ranging from fever and headache to a severe acute febrile encephalitic syndrome. A prominent feature of disease is widespread vasculitis, which leads to thrombosis, vascular occlusion, ischemia, and/or microinfarction in multiple organs, affecting the central nervous system (CNS) most severely. NiV antigens are widely detected in endothelial and smooth muscle cells of blood vessels. Abundant viral antigens are also seen in various parenchymal cells, particularly in neurons [2]. Whereas natural hosts, including pigs and cats, exhibit components of human disease (namely vasculitis), they do not develop the typical encephalitis found in humans. Several animal models, such as the hamster, ferret, and African green monkey, have been developed, mimicking more closely the disease progression in human cases. In particular, Syrian golden hamsters (*Mesocricetus auratus*) offer a small animal model that reproduces the pathology and pathogenesis of acute human NiV infection, including both respiratory and encephalitic disease [3].

METHODS

A recombinant NiV with the addition of an open reading frame encoding a fluorescent protein (mCherry) retains pathogenicity in the hamster model [4]. Employing a similar approach, we generated a recombinant NiV-Malaysia expressing ZsGreen1 (ZsG; designated here as rNiV-M/ZsG) by incorporating the ZsG open reading frame into the NiV M gene and expressing both proteins via P2A cleavage [5]. To investigate the relationship between clinical signs at disease end point and in situ NiV distribution, 60 female HsdHan: AURA golden Syrian hamsters (Envigo No. 8903F; 5 weeks of age) were inoculated intranasally, in experimental groups of 8–9 animals, with recombinant NiV-Malaysia (NiV-M; 10^5 or 10^7 50% tissue culture infective dose [$TCID_{50}$]), recombinant NiV-M/ZsG (10^5 or 10^7 $TCID_{50}$), or low passage prototype NiV-Malaysia (10^3, 10^5, or 10^7 $TCID_{50}$; Supplementary Figure 1). Five hamsters were inoculated with Dulbecco's Modified Eagle's Medium (DMEM) alone as controls. Weight, temperature, and clinical signs were assessed daily for 27 days post infection (dpi). Clinical signs were quantified by the following scoring system: 2 points each for quiet/dull/responsive disposition, hunched back/ruffled coat, hypoactivity, or mild neurological signs (abnormal gait or mild head tilt); 3 points for dehydration/decreased skin turgor; 5 points each for dyspnea, hypothermia (<34°C), or moderate neurological signs (moderate head tilt, tremors, ataxia, and/or circling); and 10 points each for inability to bear weight, frank hemorrhage, severe neurological signs (severe head tilt, seizures), or weight

Correspondence: J. R. Spengler, DVM, PhD, MPH, Centers for Disease Control and Prevention, 1600 Clifton Road, MS H18-SB, Atlanta, GA 30333 (JSpengler@cdc.gov).

The Journal of Infectious Diseases® 2020;221(S4):S448–53

DOI: 10.1093/infdis/jiz393

loss >25% baseline (at −1 dpi). Animals with a score of ≥ 10 or at completion of study (28 dpi) were humanely euthanized with an isoflurane vapor overdose.

At euthanasia, ZsG fluorescence in rNiV-M/ZsG-infected animals was visualized and imaged in situ using a Canon PowerShot G12 camera in conjunction with a Dark Reader camera filter (No. AF580), Dark Reader Spot Lamp (No. SL 10S), Dark Reader Hand Lamp (No. HL34T), and Dark Reader glasses (No. AG16), all from Clare Chemical Research (Dolores, CO).

RNA was extracted from blood and homogenized tissue samples using the MagMAX-96 Total RNA Isolation Kit (Thermo Fisher Scientific, Waltham, MA) on a 96-well ABI MagMAX extraction platform with a DNaseI treatment step according to manufacturer's instructions. RNA was quantitated using a one-step real-time polymerase chain reaction (RT-PCR) targeting the N gene sequence and standardized to 18S with a SuperScript III Platinum One-Step qRT-PCR Kit (Thermo Fisher Scientific) according to manufacturer's instructions (primer and probe sequences available on request).

Lung, liver, kidney, and brain tissues positive for viral RNA by PCR were subsequently evaluated for presence of infectious virus. Tissues were weighed and homogenized in 1 mL DMEM; titers of infectious virus were determined in Vero cells and calculated as $TCID_{50}$/g. Additional information is available in the supplementary materials and methods.

RESULTS

Hamsters inoculated intranasally with NiV are reported to reach end-point criteria between 5 and 13 dpi depending on viral dose [6]. Here, animals inoculated with rNiV-M or rNiV-M/ZsG reached end-point criteria 4–17 dpi (10^7 $TCID_{50}$) or 8–16 dpi (10^5 $TCID_{50}$) (Figure 1). When analyzed by log-rank (Mantel-Cox) or Gehan-Breslow-Wilcoxon test, survival did not significantly differ between rNiV-M- and rNiV-M/ZsG-inoculated animals at either dose. In general, animals succumbing to disease early (< 6 dpi; early-onset) met euthanasia criteria almost uniformly due to respiratory distress. Animals meeting criteria between 6–9 dpi (mid-onset) had more variable clinical signs (e.g., dyspnea, hypo/hyperactivity, abnormal gait, and/or neurological signs), whereas those euthanized at 10–17 dpi (late-onset) predominantly met criteria due to severity of neurological signs. Disease signs were also seen in animals that never reached euthanasia criteria. Of the animals inoculated with 10^7 $TCID_{50}$ of rNiV-M or rNiV-M/ZsG that demonstrated clinical signs, 5 of 9 (56%) and 6 of 8 (75%) ultimately progressed to meet euthanasia criteria, respectively. Of the animals inoculated with 10^5 $TCID_{50}$ of rNiV-M or rNiV-M/ZsG that demonstrated clinical signs, 3 of 7 (43%) and 3 of 8 (38%) ultimately progressed to meet criteria, respectively. Notably, a subset of animals (16 of 60; 26.7%) with mild (e.g., hypoactivity, abnormal gait) to moderate (e.g., head tilt) clinical signs (maximum score of 6 points), appeared to improve clinically, returning to a score of 0 (13 of 16), 2 (2 of 16), or 4 (1 of 16) by study completion (Supplementary Table 1).

At euthanasia, ZsG fluorescent signal was observed in all animals that succumbed to disease and in a subset of survivors. While individual variation was noted, in general, in early-onset animals, signal was restricted to the respiratory tract (nasal turbinates/lungs) and cervical lymph nodes (Figure 2; 4 and 5 dpi). In mid-onset animals, distribution was most variable; signal was seen in the lungs at a lower intensity and was observed in lymphatic tissue in the abdominal cavity, as well as in the frontal/olfactory region of the brain in 1 animal (Figure 2; 6 and 9 dpi). In late-onset animals, large focal lesions indicated by robust fluorescence were noted in various regions of the brain but signal was undetectable in the respiratory tract or abdominal cavity (Figure 2; 16 and 17 dpi).

In animals euthanized at 4–11 dpi, viral RNA was detected in almost all tissue samples, except in 2 heart samples collected at 8 and 10 dpi. RNAemia was only detected at ≤ 8 dpi, in 8 of 30 (26.7%) animals that met euthanasia criteria. Viral RNA was not as widely distributed and levels were lower in animals euthanized at 12–17 dpi. In survivors, viral RNA was most consistently detected in the brain, although also seen at variable levels in several other organs.

Virus was isolated from the following numbers of PCR-positive samples: lung, 16 of 34 (47.1%); liver, 14 of 40 (35.0%); kidney, 9 of 31 (29.0%); and brain, 10 of 54 (18.5%). No virus was isolated from tissue samples collected after 15 dpi, regardless of RNA levels detected by PCR or severity of disease signs at euthanasia (Figure 2, Supplementary Table 1).

DISCUSSION

Here we found that animals infected with recombinant NiV-M or NiV-M/ZsG exhibited clinical signs consistent with established models of disease [6]. We observed 2 patterns of severe disease: rapidly progressing disease characterized predominantly by dyspnea, or delayed-onset illness with neurological signs. In NiV-M/ZsG-infected hamsters, we were able to visualize virus tissue distribution in situ; ZsG signal in either respiratory or neurological tissues was directly associated with the primary clinical signs. Infectious virus could only be isolated from a subset of samples demonstrating ZsG signal and/or viral RNA presence. Notably, no isolations were successful in samples obtained from animals euthanized after 15 dpi, even those with evidence of high levels of viral RNA in tissues. While variable sensitivity of virus detection modalities can explain these discrepancies, other factors may also contribute, such as the presence of an antibody response to infection (Supplementary Table 1) that has been described previously in attempts to isolate Ebola virus in clinical samples [7].

While both respiratory and neurological disease have been described in association with NiV infection, neurological disease is

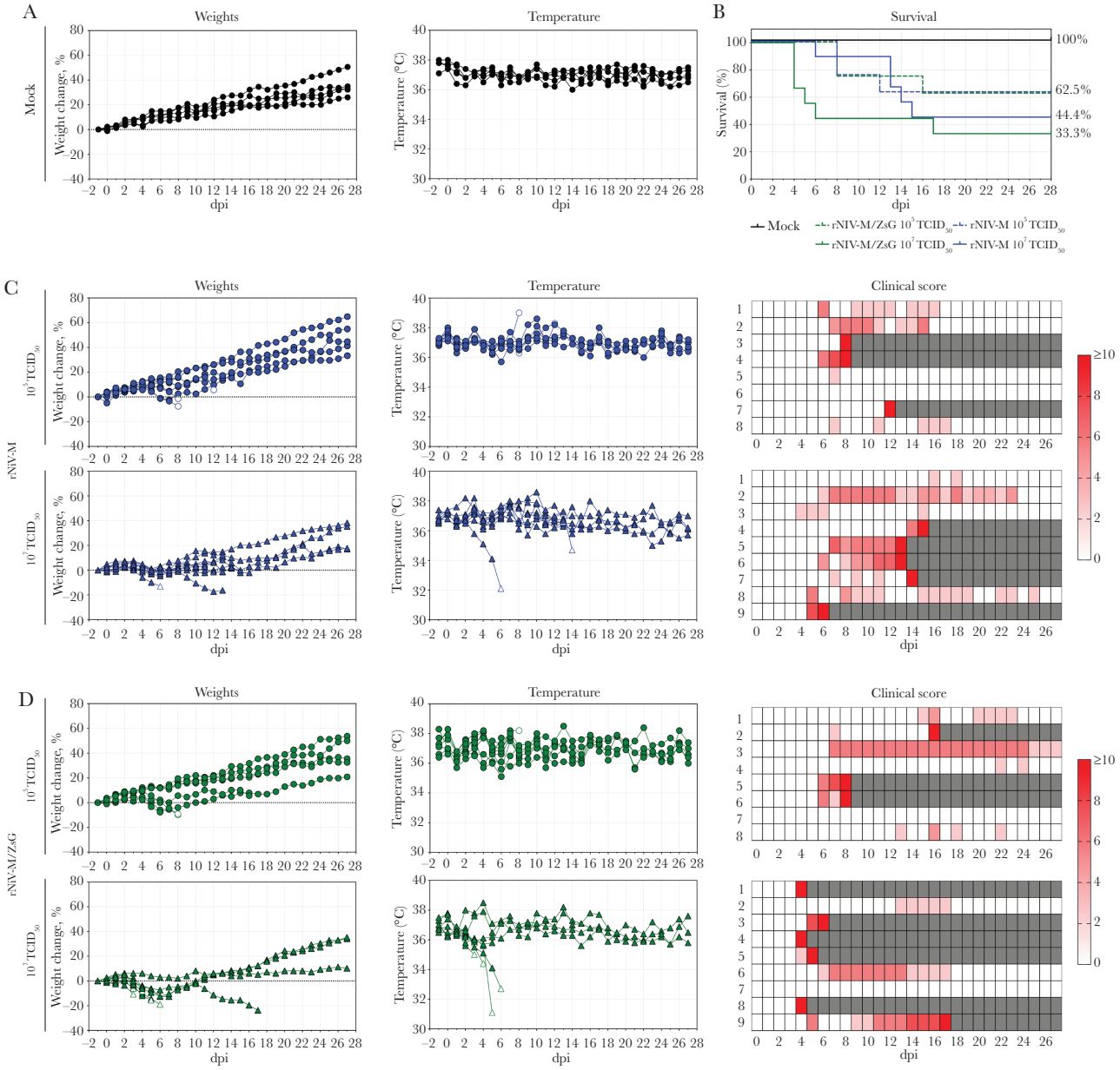

Figure 1. Mortality of hamsters inoculated with rNiV-M is comparable to mortality of hamsters inoculated with rNiV-M/ZsG. (*A*), Percent weight change from baseline (–1 dpi) and body temperatures in mock-infected (DMEM) female Syrian hamsters. (*B*), Survival of hamsters inoculated intranasally with either rNiV-M or rNiV-M/ZsG at 10^5 (n = 8, each) or 10^7 $TCID_{50}$ (n = 9, each). (*C*) and (*D*), Percent weight change from baseline (–1 dpi), body temperatures, and presence and severity of clinical signs in hamsters inoculated with (*C*) rNiV-M or (*D*) rNiV-M/ZsG. Open symbols represent the last sample obtained prior to euthanasia or succumbing to disease. Clinical signs were scored from 0 to 10, with severity depicted by increased intensity of red. Animals scoring ≥ 10 were humanely euthanized; any animals that succumbed to disease prior to euthanasia were allocated a score of 10. Grey boxes indicate the end of monitoring/scoring due to euthanasia/death. Abbreviations: DMEM, Dulbecco's Modified Eagle's Medium; dpi, days post infection; rNiV-M, recombinant Nipah virus-Malaysia; $TCID_{50}$, 50% tissue culture infective dose; ZsG, ZsGreen1 fluorescent protein.

more widely recognized. In humans, NiV causes a range of microscopic morphological changes involving primarily the central nervous system (CNS). Widespread endothelial cell infection, vasculitis, and CNS parenchymal cell infection play an essential role in the fatal outcome of human infection and appear to be central to the pathogenesis of this disease [8]. Pathological lesions in the brain of humans are quite variable [9], likely associated with areas of microinfarction. These lesions have been reported in a variety of white matter locations, including the periventricular region and corpus callosum. In addition to white matter disease, cortical lesions have also been described in patients, including brain stem involvement, and a single thalamic lesion was detected in 1 patient [10]. Here, we saw similar variability in ZsG distribution in the CNS of hamsters. Signal was detected more frequently on both the ventral surface and on sagittal cut section. We did, however, also note some less intense signal in cerebral lesions on the dorsal

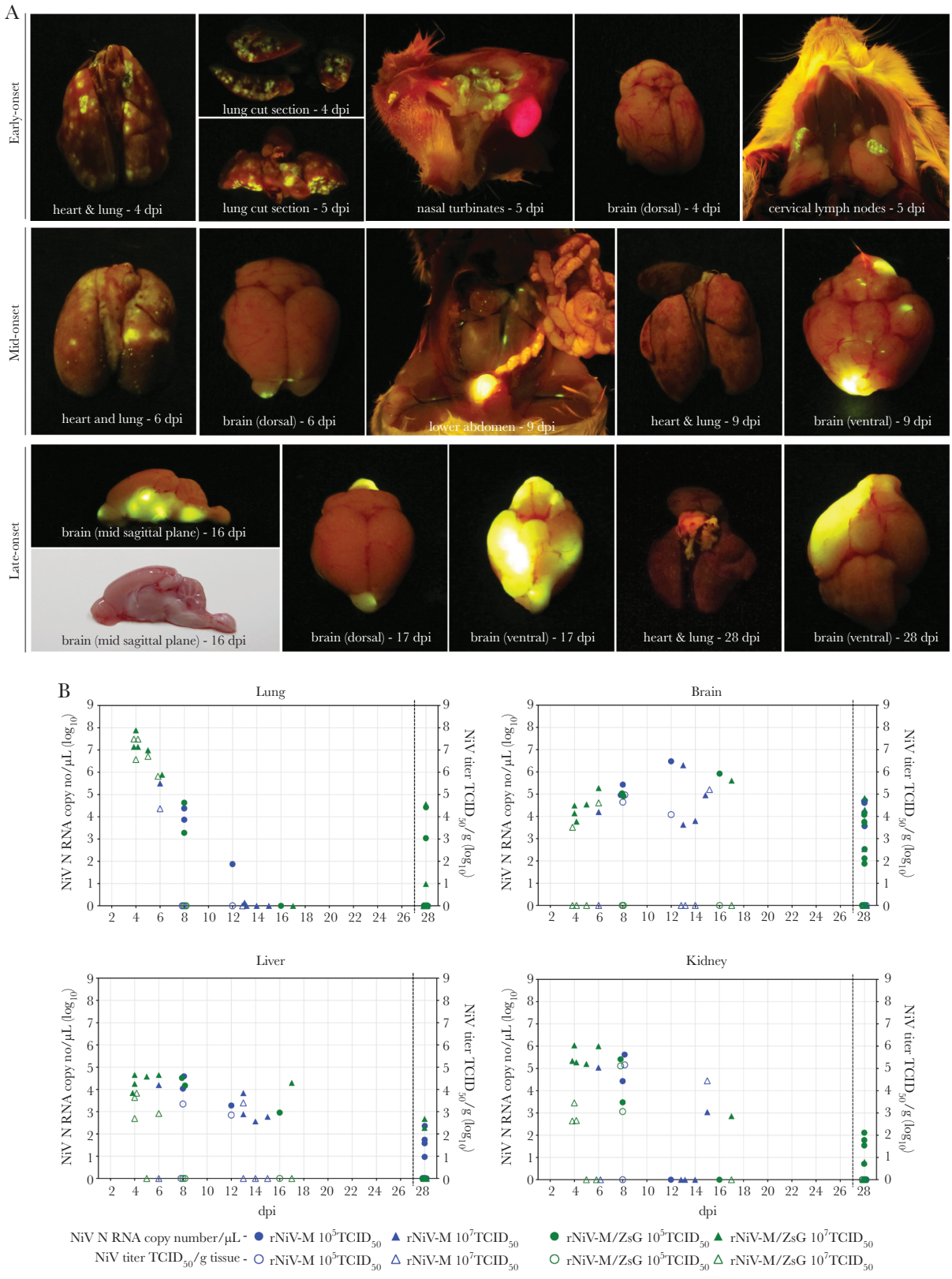

Figure 2. Visualization of ZsG signal and viral load assessment in NiV-infected hamsters. (*A*), ZsG fluorescence in lung, nasal turbinates, brain, and cervical lymph nodes of rNiV-M/ZsG-infected hamsters (10^5 or 10^7 $TCID_{50}$ IN) that succumbed to disease at early (4–5 dpi), mid (6–9 dpi), or late (16–17 dpi) timepoints after infection, and in a survivor (28 dpi). (*B*), Viral RNA (closed symbols) and isolated infectious virus (open symbols) in samples of lung, brain, liver, and kidney of hamsters inoculated IN with rNiV-M (10^5 or 10^7 $TCID_{50}$) or rNiV-M/ZsG (10^5 or 10^7 $TCID_{50}$). Abbreviations: dpi, days post infection; IN, intranasal; NiV, Nipah virus; rNiV-M, recombinant Nipah virus-Malaysia; $TCID_{50}$, 50% tissue culture infective dose; ZsG, ZsGreen1 fluorescent protein.

surface of animals that survived infection but displayed clinical signs during the study period.

In addition to neurological signs, other clinical signs are observed during human NiV disease, likely associated with the widespread pathological changes reported in cases. Similar to CNS lesions, evidence of vascular disease has also been seen in most organs examined, including the lungs, with considerable variation between cases [8]. Severe respiratory signs were more prominently described clinical characteristics of NiV infection in Bangladesh and were originally noted as distinct from clinical characteristics reported during an earlier outbreak in Malaysia and Singapore [11]. However, respiratory signs have been reported to some extent in all outbreaks; what remains unclear is the frequency and pathophysiological cause of these signs during disease. In our study, ZsG signal was detected in the respiratory tract of animals with acute severe respiratory signs and absent in those without, suggesting that the pathophysiology is dependent on viral presence, either via a direct viral-mediated effect on pulmonary tissue function or immunopathology in response to replicating virus.

Most symptomatic patients who survive acute NiV infection eventually recover without serious sequelae. However, patients can present with relapsed encephalitis months to years later or develop late-onset encephalitis [12]. In addition, imaging studies indicate that brain lesions may develop without notable clinical signs. For example, among a group of asymptomatic seropositive abattoir workers, delayed magnetic resonance imaging (MRI) revealed discrete small lesions in the brain similar to those detected in patients with symptomatic encephalitis [13]. Sejvar et al [14] studied long-term neurological and functional outcomes in a cohort of NiV-Bangladesh survivors; they found persistent neurological dysfunction in 32% of patients that survived encephalitic disease, 4 cases with delayed-onset neurological abnormalities, and evidence of MRI abnormalities in 15 of 22 cases. Neurological sequelae may also be less pronounced; 1 study following patients for 24 months found that a significant proportion of individuals developed psychiatric features, including depression and personality changes, while others had deficits in attention, verbal skills and/or visual memory [15]. Investigating disease sequelae is a valuable application of recombinant NiV expressing a foreign protein in animal models. As shown here, depending on route and dose of virus administration, a significant proportion of animals either never demonstrate overt clinical signs, despite RNA detection and/or seroconversion, or recover from clinical signs by study completion. In addition to the imaging studies to investigate acute disease, these animals represent a unique opportunity to improve our understanding of long-term disease progression and recrudescence, and, in turn, refine our approach to therapeutic evaluation and case management.

Supplementary Data

Supplementary materials are available at *The Journal of Infectious Diseases* online. Consisting of data provided by the authors to benefit the reader, the posted materials are not copyedited and are the sole responsibility of the authors, so questions or comments should be addressed to the corresponding author.

Notes

Acknowledgments. We thank Tatyana Klimova for assistance with editing the manuscript and members of the Centers for Disease Control and Prevention's Comparative Medicine Branch for providing care for the animals.

Disclaimer. The findings and conclusions in this report are those of the authors and do not necessarily represent the official position of the Centers for Disease Control and Prevention.

Financial support. This work was supported by Research Participation Program at the Centers for Disease Control and Prevention (CDC) administered by the Oak Ridge Institute for Science and Education through an interagency agreement between the US Department of Energy and CDC (S. R. W.); and by CDC Emerging Infectious Disease Research Core Funds.

Potential conflicts of interest. All authors: no reported conflicts. All authors: No reported conflicts of interest. All authors have submitted the ICMJE Form for Disclosure of Potential Conflicts of Interest. Conflicts that the editors consider relevant to the content of the manuscript have been disclosed.

References

1. Ang BSP, Lim TCC, Wang L. Nipah virus infection. J Clin Microbiol **2018**; 56:pii: e01875-17.
2. Wong KT, Shieh WJ, Kumar S, et al; Nipah Virus Pathology Working Group. Nipah virus infection: pathology and pathogenesis of an emerging paramyxoviral zoonosis. Am J Pathol **2002**; 161:2153–67.
3. Rockx B. Recent developments in experimental animal models of Henipavirus infection. Pathog Dis **2014**; 71:199–206.
4. Park A, Yun T, Hill TE, et al. Optimized P2A for reporter gene insertion into Nipah virus results in efficient ribosomal skipping and wild-type lethality. J Gen Virol **2016**; 97:839–43.
5. Lo MK, Nichol ST, Spiropoulou CF. Evaluation of luciferase and GFP-expressing Nipah viruses for rapid quantitative antiviral screening. Antiviral Res **2014**; 106:53–60.
6. Wong KT, Grosjean I, Brisson C, et al. A golden hamster model for human acute Nipah virus infection. Am J Pathol **2003**; 163:2127–37.
7. Spengler JR, McElroy AK, Harmon JR, Ströher U, Nichol ST, Spiropoulou CF. Relationship between Ebola virus real-time quantitative polymerase chain reaction-based threshold cycle value and virus isolation from human plasma. J Infect Dis **2015**; 212(Suppl 2):S346–9.
8. Hooper P, Zaki S, Daniels P, Middleton D. Comparative pathology of the diseases caused by Hendra and Nipah viruses. Microbes Infect **2001**; 3:315–22.
9. Lim CC, Sitoh YY, Lee KE, Kurup A, Hui F. Meningoencephalitis caused by a novel paramyxovirus: an advanced MRI case report in an emerging disease. Singapore Med J **1999**; 40:356–8.

10. Lim CC, Sitoh YY, Hui F, et al. Nipah viral encephalitis or Japanese encephalitis? MR findings in a new zoonotic disease. AJNR Am J Neuroradiol **2000**; 21:455–61.
11. Hossain MJ, Gurley ES, Montgomery JM, et al. Clinical presentation of Nipah virus infection in Bangladesh. Clin Infect Dis **2008**; 46:977–84.
12. Tan CT, Goh KJ, Wong KT, et al. Relapsed and late-onset Nipah encephalitis. Ann Neurol **2002**; 51:703–8.
13. Lim CC, Lee WL, Leo YS, et al. Late clinical and magnetic resonance imaging follow up of Nipah virus infection. J Neurol Neurosurg Psychiatry **2003**; 74:131–3.
14. Sejvar JJ, Hossain J, Saha SK, et al. Long-term neurological and functional outcome in Nipah virus infection. Ann Neurol **2007**; 62:235–42.
15. Ng BY, Lim CC, Yeoh A, Lee WL. Neuropsychiatric sequelae of Nipah virus encephalitis. J Neuropsychiatry Clin Neurosci **2004**; 16:500–4.